A&A 493, 1075–1080 (2009)
DOI: 10.1051/0004-6361:200810619

Astronomy & Astrophysics

Assessment of the near infrared identification of carbon stars

II. The local group galaxies IC 1613 and NGC 3109⋆,⋆⋆

P. Battinelli[1] and S. Demers[2]

[1] INAF, Osservatorio Astronomico di Roma Viale del Parco Mellini 84, 00136 Roma, Italy
e-mail: battinel@inaf.it
[2] Département de Physique, Université de Montréal, C.P. 6128, Succursale Centre-Ville, Montréal, Qc, H3C 3J7, Canada
e-mail: demers@astro.umontreal.ca

Received 16 July 2008 / Accepted 3 October 2008

ABSTRACT

Context. Thousands of C stars have been identified in Local Group galaxies using narrow band photometry. To survey C stars at larger distances and alternative to the narrow-band approach is needed.
Aims. We obtain, from ESO Archive data, NIR magnitudes and colours of previously known C stars in two dwarf irregular Local Group galaxies, namely IC 1613 and NGC 3109.
Methods. We compare the NIR magnitudes and colours of the C star populations, previously identified from narrow band techniques to estimate the star formation history of their intermediate-age populations.
Results. We demonstrate that the photometric properties of C stars show a wider range in the NIR than in the optical. As confirmed by models we see, among the four galaxies investigated with a 0.7 dex metallicity range, little if any metallicity effect in the C star colour distribution.

Key words. stars: AGB and post-AGB – stars: carbon – galaxies: dwarf

1. Introduction

In a previous paper (Battinelli et al. 2007, hereafter Paper I) we compiled near-infrared mean magnitudes and colours of carbon stars, mostly identified from narrow-band photometry, in various galaxies. We concluded that $(J - K_s)_0 = 1.4$ can be regarded as a conservative limit for the selection of C stars among the AGB population because essentially no M-type stars have such a red colour. This colour limit should not, however, be used to count C and M-type AGB stars because too many C stars do have colours bluer than the above limit and near-infrared colours are not useful to establish the C/M ratio in galaxies. Nevertheless, the NIR approach to AGB studies does appear to be a promising tool to reach distant galaxies since most of the energy output of these late-type giants is in the red.

In order to further compare the NIR properties of C stars and assess their usefulness as near-infrared standard candles, we continue our survey of nearby galaxies. To do so, we searched the ESO archives for SOFI or ISAAC observations of Local Group galaxies. We present here NIR magnitudes and colours of previously known C stars in IC 1613 and NGC 3109.

1.1. The target galaxies

Luminosity wise, with $M_v = -14.9$, IC 1613 ranks 6th among the 15 dwarf irregular (dIrr) galaxies of the Local Group, being between NGC 3109 and Sextans A. Its distance has been accurately determined by Dolphin et al. (2001), from the apparent magnitudes of the red giant branch tip (TRGB) and of the red clump stars, who obtained $\mu_o = 24.31 \pm 0.06$ (730 ± 20 kpc). Pietrzyński et al. (2006a) determined the IC 1613 distance to be $\mu_o = 24.291 \pm 0.014$ (720 ± 5 kpc), from near infrared photometry of its Cepheids. Based on these two estimates, we adopt 722 ± 5 kpc for the distance of IC 1613. The foreground reddening is taken to be $E(B - V) = 0.03$, corresponding to $E(J - K_s) = 0.016$. IC 1613 is essentially a typical irregular galaxy. Albert et al. (2000), using the narrow-band index (CN – TiO), identified some 200 C stars extending to 15′ from the center of IC 1613. This result not surprising since the NIR observations of IC 1613 obtained by Borissova et al. (2000) revealed that the galaxy has a rich intermediate-age AGB population. According to Skillman et al. (2003), IC 1613 has a relatively constant star formation rate over the age of the Universe.

Recently, Zucker & Wyder (2004), using DEIMOS at the Keck telescope, determined the metal abundance of numerous RGB stars in IC 1613. The mean abundance, based on the equivalent width of the CaII triplet, is quoted as [Fe/H] = –1.3. This value is in good agreement with the Skillman et al. (2003) SFH models which suggest an abundance of [Fe/H] ≈ –1.0 for the intermediate-age stars.

NGC 3109, an outlying member of the Local Group, is a southern hemisphere dwarf irregular galaxy, more luminous and more massive than IC 1613. Because of its proximity to us it turns out to be one of the brightest galaxies seen in the southern sky. Its carbon star population has been surveyed by Demers et al. (2003) who identified over 400 C stars using the narrow band technique. Recently the near-infrared J and K_s magnitudes of 77 Cepheids have been used by Soszyński et al. (2006) to accurately determine the distance of NGC 3109. We adopt their estimates, $(m-M)_0 = 25.57 \pm 0.024$ along with $E(B-V) = 0.09$,

⋆ This publication makes use of data products from the ESO Archive.
⋆⋆ Full Tables 2 and 3 are only available in electronic form at http://www.aanda.org

Table 1. Fields observed in each galaxy.

Galaxy	RA J2000	Dec
IC 1613 F1	01:04:57.0	+02:08:36
IC 1613 F2	01:04:40.5	+02:08:37
IC 1613 F3	01:04:52.3	+02:03:50
NGC 3109 F1	10:03:18.3	–26:09:18
NGC 3109 F2	10:03:08.0	–26:10:10
NGC 3109 F3	10:02:58.4	–26:09:53

or $E(J-K_s) = 0.048$ and $A_K = 0.03$. Alonso et al. (1999) published NIR observations of NGC 3109. However, their data are not deep enough for a full assessment of the intermediate-age population. The metallicity of the old population of NGC 3109 has been estimated by Mendez et al. (2002) from the $(V-I)_{0,\mathrm{TRGB}}$ to be [Fe/H] $= -1.69 \pm 0.06$.

2. Observations and data reduction

2.1. IC 1613

The J and K_s observations of IC 1613 were obtained from the ESO Archive. They consist of NTT data, from La Silla, obtained with the SOFI near infrared camera in September 2004 as part of the Araucaria Cepheid project (Pietrzyński et al. 2006a). The field of SOFI is $4.9' \times 4.9'$ and the scale is 0.288 arcsec per pixel. The coordinates of the three fields, read from the image header, are given in Table 1. Details of these observations are described by Pietrzyński et al. (2006a). In the K_s filter, they obtained six consecutive 10 s integrations at a given position and then moved the telescope by about $20''$ to a different random position. Integrations obtained at 65 different dithering positions resulted in a total exposure time of 65 min in the K_s filter for a given field. For the J filter for which the sky shows less variation, two consecutive 20 s exposures were obtained for 25 dithering positions for a total of 17 min on a given field.

The raw images obtained from the Archives were reduced using the XDIMSUM task in IRAF. The resulting combined images were analysed with DAOPHOT and ALLSTAR. After obtaining the astrometric solution for one image in each field we match the stars found with the 2MASS catalogue. The zero point adjustments between our instrumental magnitudes and the 2MASS magnitudes are based on about six stars per field, excluding the fainter 2MASS stars with large uncertainties. The standard deviations of the differences between the 2MASS magnitudes and our instrumental magnitudes are ± 0.08 for K_s and ± 0.07 for J. The J zero points for the three fields as well as those in K_s of F1 and F2 agree within the errors, while the K_s zero point of F3 differs by 0.6 mag.

Further assessment of the reliability of our photometry can be done by comparing the magnitudes of the stars in the overlapping region between field F1 and F2. We calculate, for 45 stars, $\Delta K_s = -0.06 \pm 0.10$; a somewhat larger difference is found for J but with the same dispersion.

2.2. NGC 3109

The NGC 3109 images are also extracted from the ESO Archives. They were obtained with ISAAC at the VLT by Soszyński et al. (2006) as part of the Araucaria project. They observed three $2.5' \times 2.5'$ fields in J and K_s bands; the scale is $0.147''$ per pixel. The reader is referred to the above publication for further observation details. We reduce the raw images using JITTER from the ECLIPSE package developed by ESO. The combined images were then analysed with DAOPHOT and ALLSTAR.

The small size of the images makes the astrometric and magnitude calibrations more difficult than for the SOFI data. For the astrometry we use as a reference the C star coordinates published by Demers et al. (2003) and seen in the field. Because of the lack of suitable 2MASS stars, the magnitude calibration is done using the published J and K_s magnitudes of the Cepheids (Soszyński et al. 2006), taken on the same night as the images we analyse. The Cepheid coordinates are listed by Pietrzyński et al. (2006b). We first adjust the magnitude zero points of field F1 and F3 to those of F2 by comparing the magnitudes of stars in the overlapping regions. We then use the published magnitudes of 36 Cepheids with $K_s < 20.0$ seen within the three fields to calibrate the instrumental magnitudes. From this comparison we obtain $\sigma_K = \pm 0.18$ and $\sigma_J = \pm 0.09$ mag. The J2000 equatorial coordinates of the NGC 3109 fields are given in Table 1.

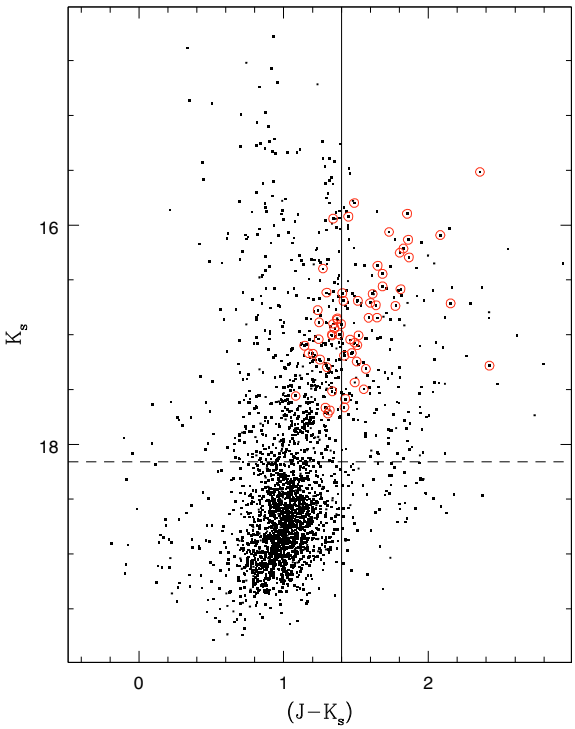

Fig. 1. The colour–magnitude diagram of the combined three IC 1613 fields. The circles correspond to the known C stars identified from narrow-band photometry. The dashed line is at the TRGB level and the vertical lines marks the $J - K_s = 1.4$ limit.

3. Results

3.1. IC 1613

The colour–magnitude diagram of the combined three SOFI fields of IC 1613 is displayed in Fig. 1. Sixty one C stars identified by Albert et al. (2000) are matched to the stars above the TRGB in our NIR photometry. Their NIR magnitude and colour are given in Table 2. The identification numbers are those assigned by Albert et al. (2000). Among the 61 stars matched, only 37 (61%) of them have $(J-K_s) > 1.4$. If we assume that all AGB stars above the TRGB and with $(J - K_s) > 1.4$ are C stars, then there are 190 such objects in our IC 1613 fields.

Table 2. NIR magnitudes and colours of C stars in IC 1613[a].

id	RA	Dec	K_s	σ_K	$J-K_s$	σ_{J-K}
39	1:04:30.50	2:06:47.7	17.516	0.015	1.336	0.021
49	1:04:33.90	2:08:31.3	15.941	0.009	1.342	0.017
50	1:04:34.00	2:06:00.6	16.627	0.012	1.615	0.021
51	1:04:34.50	2:10:09.5	16.999	0.012	1.333	0.018
54	1:04:35.30	2:06:06.1	16.942	0.012	1.352	0.020
55	1:04:35.40	2:06:54.4	16.904	0.011	1.397	0.016
56	1:04:35.60	2:08:31.3	16.371	0.009	1.650	0.017
57	1:04:36.60	2:06:39.7	16.134	0.009	1.861	0.014
60	1:04:37.10	2:07:47.4	17.244	0.013	1.505	0.019
62	1:04:37.40	2:07:39.9	17.168	0.011	1.471	0.018
63	1:04:37.40	2:09:40.1	17.006	0.012	1.336	0.021

[a] Table 2 is presented in its entirety in the electronic edition of the journal. A portion is shown here for guidance regarding its form and content.

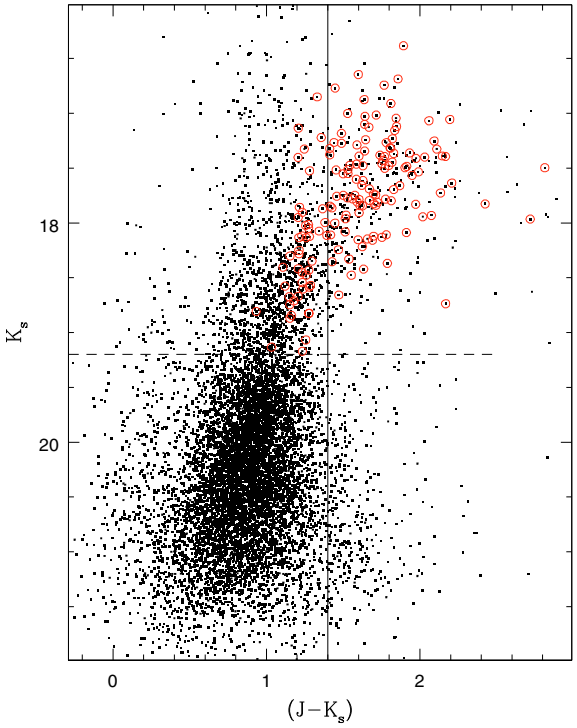

Fig. 2. CMD of the three fields of NGC 3109. The dashed line traces the level of the TRGB and the vertical lines is at $(J-K_s) = 1.4$. The matched C stars are circled.

3.2. NGC 3109

The colour magnitude diagram of the combined three ISAAC fields of NGC 3109 is presented in Fig. 2. 157 C stars were cross-identified with our optical photometry (Demers et al. 2003); a few stars are found in more than one ISAAC fields. They are identified by circles on the CMD of Fig. 2. We list, in Table 3, the NIR magnitude and colour of the C stars. The identification numbers are from Demers et al. (2003). Among the 157 stars matched, 111 of them (71%) have $(J-K_s) > 1.4$ If, similarly to IC 1613, we call all the AGB redder than 1.4 C stars, then we count 310 such stars in the NGC 3109 fields. The interpretation of these numbers is difficult. For example, a comparison of Figs. 1 and 2 reveals an abnormal number of faint red stars in the IC 1613 CMD, at the TRGB level, not seen in NGC 3109. The nature of the stars with $(J-K_s) > 1.4$ cannot be confirmed by our optical photometry because we do not have equatorial coordinates for either of the full databases.

Table 3. NIR magnitudes and colours of C stars in NGC 3109[a].

id	RA	Dec	K_s	σ_K	$J-K_s$	σ_{J-K}
106	10:02:53.17	–26:09:08.2	18.023	0.031	1.255	0.048
108	10:02:53.92	–26:10:20.1	17.550	0.037	1.531	0.056
109	10:02:54.11	–26:10:33.2	17.514	0.043	1.532	0.056
111	10:02:54.29	–26:09:57.8	18.843	0.040	1.163	0.047
112	10:02:54.59	–26:10:02.5	18.081	0.025	1.513	0.029
113	10:02:54.74	–26:08:52.1	18.477	0.035	1.260	0.043
116	10:02:54.90	–26:10:34.8	18.586	0.038	1.278	0.048
117	10:02:55.24	–26:09:13.0	18.302	0.023	1.154	0.026
118	10:02:55.40	–26:09:19.2	18.868	0.033	1.153	0.038
119	10:02:55.42	–26:10:59.8	17.997	0.038	1.382	0.054
122	10:02:55.95	–26:08:37.6	18.403	0.045	1.108	0.060
123	10:02:56.59	–26:08:54.7	17.477	0.021	1.797	0.028

[a] Table 3 is presented in its entirety in the electronic edition of the journal. A portion is shown here for guidance regarding its form and content.

4. Discussion

4.1. C stars in the CMD

Since the regions observed in NGC 3109 and IC 1613 contain numerous Cepheids we must conclude that we are dealing with populations of mixed ages. In Fig. 3 we draw the Cioni et al. (2006) published isochrones of AGB models on the colour-magnitude diagram of the known C stars in IC 1613. We prefer these isochrones to those of Marigo et al. (2008) because the latter do not reach $(J-K_s)$ colours as red as the C stars observed. We select a metallicity of $Z = 0.001$, the most appropriate for the adopted abundance. The youngest C stars have an age of ∼400 Myr while the bulk of the C star population is between 700 Myr and 2.5 Gyr. Some faint C stars can be explained by a lower metallicity as shown by the dashed line (corresponding to 2.5 Gyr and $z = 0.0004$). A similar plot for NGC 3109, with its adopted lower metallicity, is presented in Fig. 4. Here we see that all C stars were formed between 250 Myr and 2.5 Gyr ago. Again we note that SFH has been variable during that interval. More than half the C stars are between 500 and 800 Myr old.

The C star population in the galaxies discussed in Paper I can likewise be compared, selecting the proper abundances. We display in Fig. 5 the CMDs of C stars in IC 10, NGC 6822 and WLM. The NGC 6822 data are taken from Kang et al. (2006). The SFH of the intermediate age population is similar in the three galaxies with the oldest star being some 2.5 Gyr old and the youngest close to half a Gyr.

4.2. Colour distribution of C stars

We remarked in Paper I that C stars are found over a wide range of NIR colours. We compare, in Fig. 6, the $(J-K_s)_0$ colour distributions of C and M stars, previously identified from our RICNTiO photometry in four dwarf galaxies: IC 1613 and NGC 3109 which NIR are presented here, and WLM from Paper I and NGC 6822 with NIR from Kang et al. (2006). We omit here IC 10 because of its extreme and ill-defined colour excess. Stars with positive (CN – TiO) are C stars while those with a negative index are M stars which could be giants in the galaxy or dwarf M stars seen along the line of sight. The

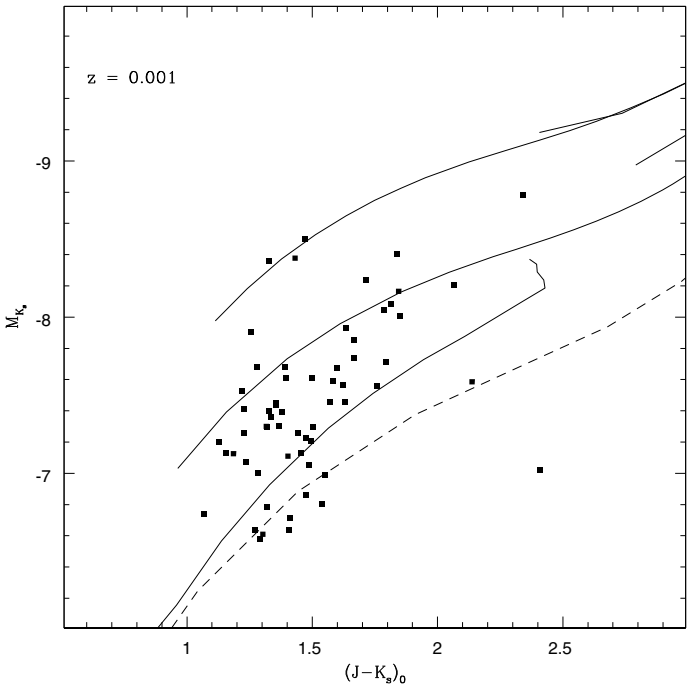

Fig. 3. CMD of known C stars in IC 1613. The isochrones of Cioni et al. (2006) indicate that C stars were formed between 400 Myr and 2.5 Gyr ago. The bulk of the C stars were formed more than 700 Myr ago. The dashed isochrone corresponds to $z = 0.0004$.

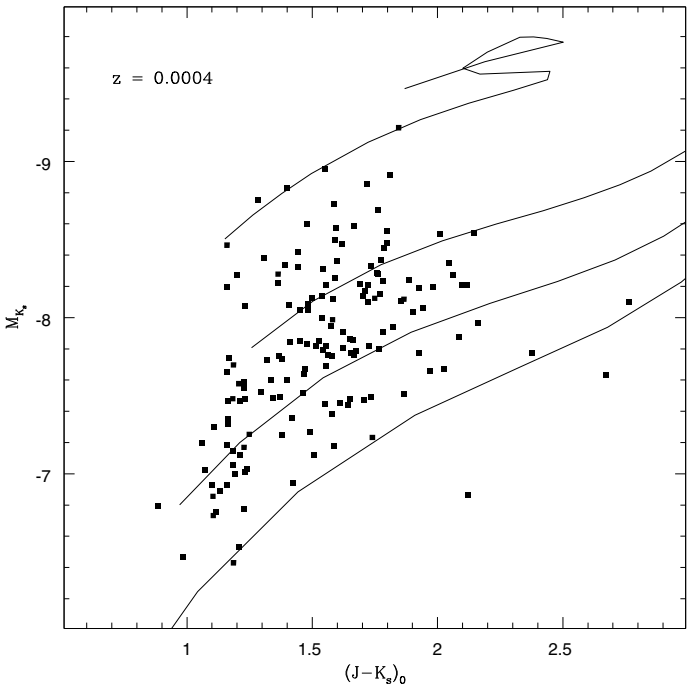

Fig. 4. CMD of known C stars in NGC 3109. The isochrones correspond, *from top to bottom*, to ages of 0.25, 0.5, 0.8 and 2.5 Gyr.

narrow band technique can, however, discriminate only stars with $(R - I) > 0.9$, a colour limit corresponding to N-type C stars. We adopted, in Paper I, $(J - K_s)_0 = 1.40$ as the working limit to separate C and M stars. We see, from the vertical lines drawn in Fig. 6, that this limit corresponds essentially to the red border of the M stars but certainly not to the blue border of C stars.

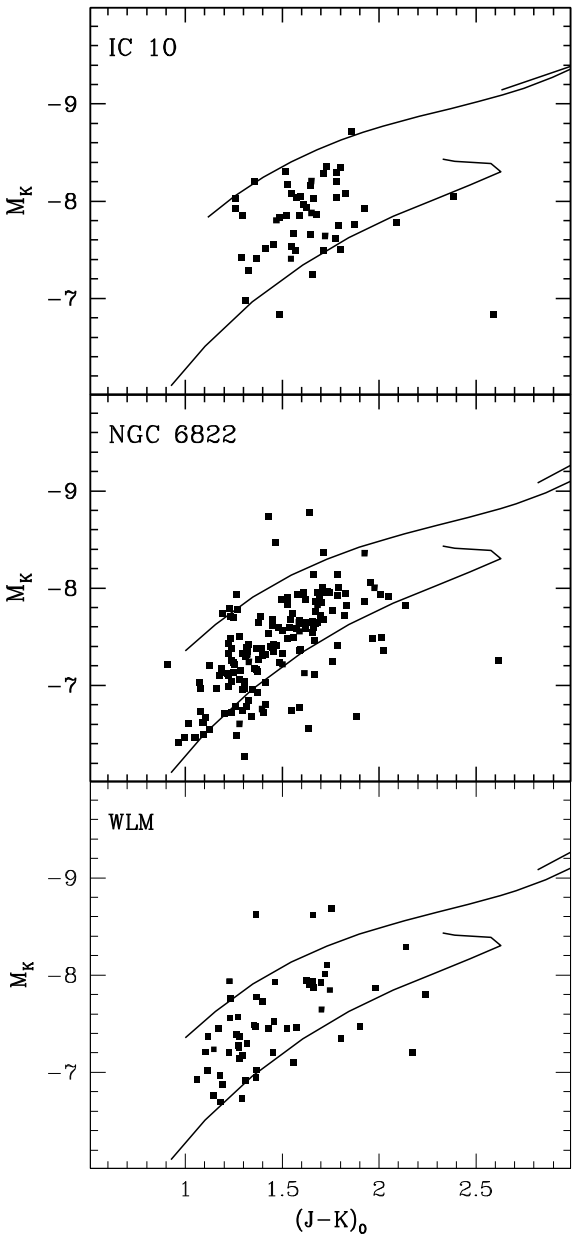

Fig. 5. CMD of known C stars in IC 10, NGC 6822 and WLM. The lower isochrones correspond to 2.5 Gyr while the top ones represent, respectively, 450 Myr (IC 10), 560 Myr (NGC 6822) and 560 Myr (WLM).

Various authors (Davidge 2003; Cioni & Habing 2003; Cioni & Habing 2005; Valcheva et al. 2007) have shifted the blue limit of C stars to take into account the metallicity of the galaxy under consideration. The metallicity of the intermediate-age populations of Local Group galaxies is in general rather poorly known. High resolution spectroscopy has recently target young giants in a few LG dwarf irregulars while the equivalent width of the CaII triplet has been used to infer the abundance of old red giants. The intermediate-age populations of the four galaxies displayed in Fig. 6 show a rather narrow range of metallicities. We adopted earlier for IC 1613 and NGC 3109 respectively [Fe/H] = –1.0 and –1.69, while Battinelli & Demers (2005) adopted –1.4 for WLM and –1.25 for NGC 6822. The C star distributions in the $(CN - TiO) - (J - K_s)$ plane are surprisingly similar, with possibly an exception in the case of NGC 6822 where a "blue C star branch" is seen going toward $(CN - TiO) = 0.0$. The numbers

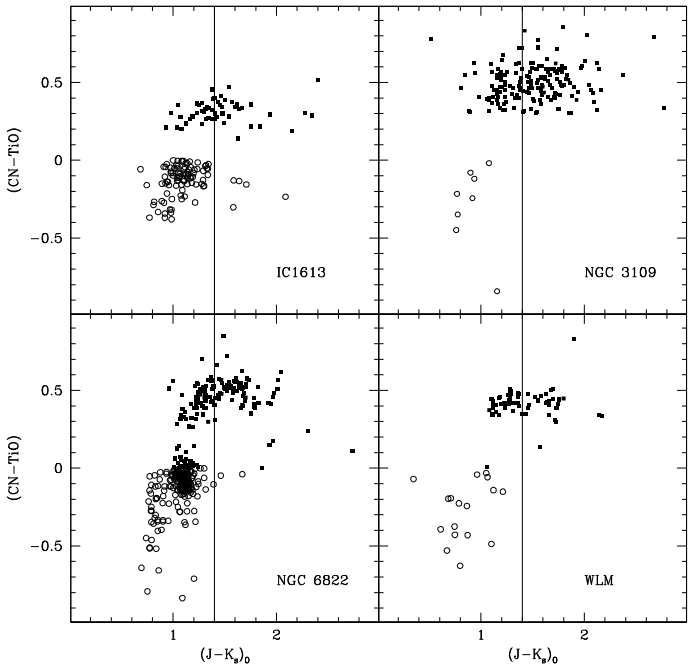

Fig. 6. C (filled squares) and M stars (open circles) as defined from RICNTiO photometry have NIR colours that overlap. The vertical lines trace the $(J - K_s)_0 = 1.4$ limit.

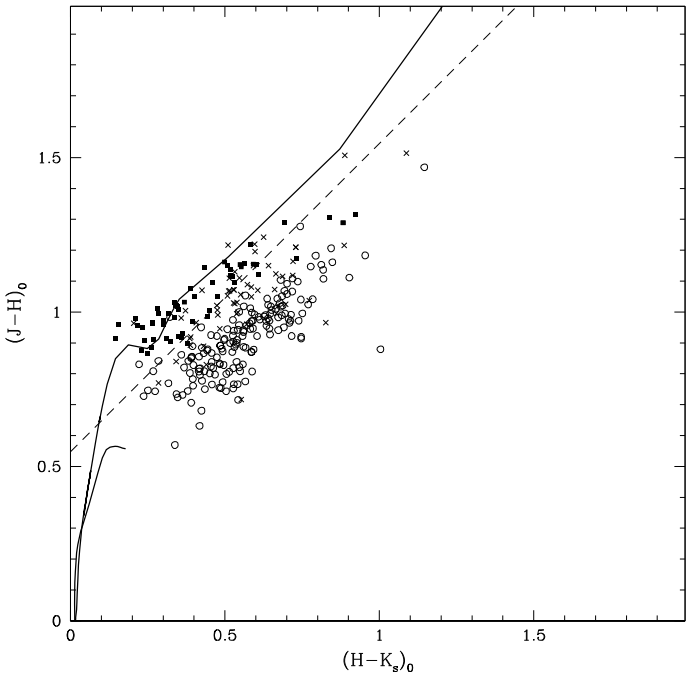

Fig. 7. Known C stars in WLM (black squares), IC 10 (crosses) and NGC 6822 (circles) are clearly separated. The dashed line represents Whitelock et al. (2006) regression. The curve is a typical 1 Gyr isochrone.

of C stars plotted depend on the size and stellar density of the regions surveyed. Thus, we see little metallicity effect here.

4.3. C stars on the colour–colour diagram

Whitelock et al. (2006) have investigated the NIR colours of Galactic and Magellanic C stars. They conclude that individual members of the two populations cannot be distinguished from their position in the $(J - H)$ vs. $(H - K_s)$ plane. We do not have H magnitudes for the C stars observed in NGC 3109 and IC 1613 but such data are available for IC 10, WLM and NGC 6822 discussed in Paper I. We are then in a position to compare their locations on the colour-colour diagram. The NIR colours of known C stars identified from the (CN − TiO) index in these three galaxies are plotted in Fig. 7. The dashed line is the Whitelock et al. (2006) regression. We draw a representative isochrone from Marigo et al. (2008) for 1 Gyr, $z = 0.001$. Isochrones of different metallicities nearly coincide, proving that there is no appreciable shift with abundance. We observe that the data points of WLM and IC 10 essentially overlap, while those of NGC 6822 are offset. Since NGC 6822 contains numerous C stars it would be useful to obtain an independent dataset to confirm this shift.

Jackson et al. (2007a) in their Spitzer observations of WLM state that only 18% of the AGB C stars were detected by the (CN − TiO) approach. This number is somewhat misleading; as explained later by Jackson et al. (2007b), the narrow band technique can only detect the subsample C stars with $(R - I) > 0.90$ that corresponds to the N-types. In Fig. 8 we cross identify our NIR data of the AGB stars of IC 1613 with the Spitzer data to produce a colour–colour diagram. The C stars identified from their (CN − TiO) index by Albert et al. (2000) are also cross identified with the NIR observations. We see that there are, as expected, few C stars bluer than $(J - K_s) \approx 1.4$. There are also few C stars among the AGBs that have a positive [3.6] – [4.5] Spitzer index, presumably because these stars were too faint in the optical to be included in the Albert et al. list.

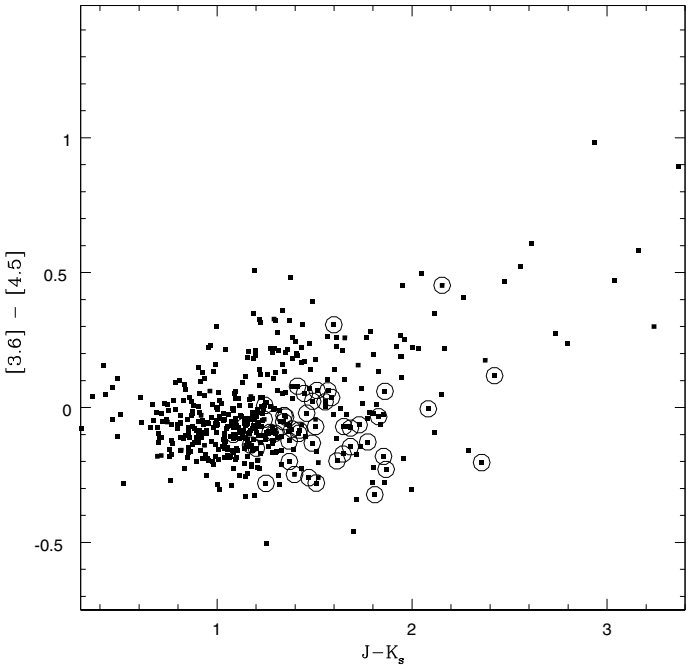

Fig. 8. Colour–colour diagram of the AGB stars in IC 1613. The circled dots are C stars identified by the narrow-band technique.

5. Conclusion

The photometric approach to identifying C stars from M giants leads to different results when one adopts the optical narrow-band rather than the NIR colours.

The (CN − TiO) narrow-band technique has been successful in separating C stars and M giants, providing that their $(R - I)_0$ colour is higher than 0.90. In that colour range one finds the N-type C stars. The blue hotter C stars cannot be isolated from

late K or early M stars because they have nearly the same (CN − TiO) index.

The N-type C stars, however, show a range of $(J - K_s)$ colours, overlapping substantially with M stars. Comparison of the C and M sample, obtained from the (CN−TiO), reveals, however, that very few M stars have $(J - K_s) > 1.4$, as can be seen in Fig. 6. Thus, this limit can be adopted as a working threshold for the detection of C stars. The determination of the C/M ratio on the basis of the $(J - K_s)$ colour selection of AGB stars leads to a ratio that differs from the one calculated from the narrow-band identification. Furthermore, the determination of the number of AGB M stars requires the adoption of a blue colour limit in $(J - K_s)$ to exclude the K-type AGB stars.

The effect of the metallicity on the above threshold is not yet fully demonstrated because our small galaxy sample does not cover a wide range of abundances. In this respect, the comparison of our narrow band survey of the low metallicity Sagittarius dwarf irregular galaxy (Demers & Battinelli 2002) with the recently published NIR observations of Gullieuszik et al. (2007) could be useful to see if a metallicity effect is present. At the other abundance extreme, the narrow band survey of the outer disk of M 31 by Battinelli & Demers (2003) should be repeated in the NIR.

Acknowledgements. This research is funded by the Natural Sciences and Engineering Research Council of Canada. We are grateful to Dr. Dale Jackson for providing the Spitzer data.

References

Albert, L., Demers, S., & Kunkel, W. E. 2000, AJ, 119, 2780
Alonso, M. V., Minniti, D., Zijlstra, A. A., & Tolstoy, E. 1999, A&A, 346, 33
Battinelli, P., & Demers, S. 2003, AJ, 125, 1298
Battinelli, P., & Demers, S. 2005, A&A, 434, 657
Battinelli, P., Demers, S., & Mannucci, F. 2007, A&A, 474, 35 (Paper I)
Bellazzini, M., Ferraro, F. R., Sollima, A., et al. 2004, A&A, 424, 199
Brewer, J. P., Richer, H. B., & Crabtree, D. R. 1996, AJ, 112, 491
Borissova, J., Georgiev, L., Kurtev, R., et al. 2000, Rev. Mex. Astron. Astrofis., 36, 151
Cioni, M.-R. L., & Habing, H. J. 2003, A&A, 402, 133
Cioni, M.-R. L., & Habing, H. J. 2005, A&A, 429, 837
Cioni, M.-R. L., Girardi, L., Marigo, P., & Habing, H. J. 2006, A&A, 448, 77
Davidge, T. J. 2003, ApJ, 597, 289
Demers, S., & Battinelli, P. 2002, AJ, 123, 238
Demers, S., Battinelli, P., & Letarte, B. 2003, A&A, 410, 795
Dolphin, A. E., Saha, A., Skillman, E. D., et al. 2001, ApJ, 550, 554
Dolphin, A., et al. 2005, see http://purcell.as.arizona.edu/pubs/cancun.ps.gz
Gullieuszik, M., Rejkuba, M., Cioni, M. R., Habing, H. J., & Held, E. V. 2007, A&A, 475, 467
Jackson, D. C., Skillman, E. D., Gehrz, R. D., et al. 2007a, ApJ, 656, 818
Jackson, D. C., Skillman, E. D., Gehrz, R. D., et al. 2007b, ApJ, 667, 891
Kang, A., Sohn, Y.-J., Kim, H.-L., et al. A&A, 454, 717
Lee, M. G. 1993, ApJ, 408, 409
Marigo, P., Girardi, L., Bressan, A., et al. 2008, A&A, 482, 883
Mendez, B., Davis, M., Moustakas, J., et al. 2002, AJ, 124, 213
Pietrzyński, G., Gieren, W., Soszyński, I., et al. 2006a, ApJ, 642, 216
Pietrzyński, G., Gieren, W., Udalski, A., et al. 2006b, ApJ, 648, 366
Skillman, E. D., Tolstoy, E., Cole, A. A., et al. 2003, ApJ, 596, 253
Soszyński, I., Geiren, W., Pietrzyński, G., et al. 2006, ApJ, 648, 375
Valcheva, A. T., Ivanov, V. D., Ovcharov, E. P., & Nedialkov, P. L. 2007, A&A, 466, 501
Whitelock, P. A., Feast, M. W., Marang, F., & Groenewegen, M. A. T. 2006, MNRAS, 369, 751
Zucker, D. B., & Wyder, T. K. 2004, in Origin and Evolution of the Elements, a Carnegie Observatories Astrophysics Series, 4, ed. A. McWilliam, & M. Rauch (Pasadena: Carnegie Observatories, http://www.ociw.edu/ociw/symposia/series/symposium4/proceedings.html

Table 2. NIR magnitudes and colours of C stars in IC 1613.

id	RA	Dec	K_s	σ_K	$J-K_s$	σ_{J-K}
39	1:4:30.50	2:6:47.7	17.516	0.015	1.336	0.021
49	1:4:33.90	2:8:31.3	15.941	0.009	1.342	0.017
50	1:4:34.00	2:6:0.6	16.627	0.012	1.615	0.021
51	1:4:34.50	2:10:9.5	16.999	0.012	1.333	0.018
54	1:4:35.30	2:6:6.1	16.942	0.012	1.352	0.020
55	1:4:35.40	2:6:54.4	16.904	0.011	1.397	0.016
56	1:4:35.60	2:8:31.3	16.371	0.009	1.650	0.017
57	1:4:36.60	2:6:39.7	16.134	0.009	1.861	0.014
60	1:4:37.10	2:7:47.4	17.244	0.013	1.505	0.019
62	1:4:37.40	2:7:39.9	17.168	0.011	1.471	0.018
63	1:4:37.40	2:9:40.1	17.006	0.012	1.336	0.021
65	1:4:38.50	2:8:22.3	16.091	0.008	2.083	0.016
66	1:4:38.50	2:9:40.2	16.620	0.011	1.406	0.020
67	1:4:38.80	2:8:54.0	17.662	0.012	1.421	0.019
68	1:4:39.00	2:8:45.1	17.073	0.014	1.490	0.025
69	1:4:39.50	2:10:10.4	17.006	0.013	1.518	0.020
70	1:4:39.80	2:9:13.9	16.900	0.011	1.344	0.017
71	1:4:39.90	2:9:52.7	17.436	0.011	1.492	0.018
73	1:4:40.10	2:7:40.0	16.062	0.010	1.729	0.018
74	1:4:40.10	2:8:45.4	16.844	0.011	1.646	0.018
76	1:4:40.70	2:7:25.4	17.191	0.011	1.419	0.018
78	1:4:41.00	2:7:7.1	17.094	0.015	1.509	0.023
79	1:4:41.70	2:9:57.6	17.296	0.013	1.299	0.020
81	1:4:41.90	2:8:36.9	17.665	0.013	1.289	0.019
82	1:4:41.90	2:10:2.5	16.731	0.010	1.638	0.017
85	1:4:42.30	2:8:16.9	16.737	0.010	1.773	0.018
86	1:4:42.50	2:10:26.0	17.586	0.013	1.426	0.021
88	1:4:42.70	2:8:56.6	15.515	0.009	2.357	0.016
89	1:4:43.30	2:2:9.7	16.887	0.016	1.245	0.019
90	1:4:43.30	2:6:4.5	17.174	0.013	1.202	0.019
92	1:4:43.60	2:8:20.1	16.295	0.010	1.867	0.017
93	1:4:44.40	2:8:9.7	16.585	0.009	1.809	0.016
94	1:4:44.50	2:3:44.5	16.714	0.013	2.154	0.022
95	1:4:44.70	2:7:11.9	17.497	0.012	1.554	0.019
97	1:4:45.40	2:4:38.3	17.169	0.018	1.172	0.022
98	1:4:46.00	2:10:28.3	17.719	0.013	1.306	0.020
99	1:4:47.30	2:8:36.0	16.252	0.007	1.802	0.011
100	1:4:47.70	2:6:29.0	17.041	0.011	1.242	0.017
101	1:4:47.70	2:8:15.4	15.897	0.008	1.854	0.016
102	1:4:48.20	2:6:5.5	16.709	0.012	1.599	0.021
103	1:4:48.50	2:5:16.3	16.214	0.011	1.828	0.017
104	1:4:49.20	2:3:26.3	16.851	0.013	1.370	0.018
107	1:4:50.20	2:6:39.0	16.690	0.015	1.513	0.026
108	1:4:50.30	2:4:47.1	15.923	0.011	1.448	0.015
111	1:4:50.60	2:3:42.1	16.616	0.013	1.297	0.018
113	1:4:51.40	2:10:41.7	16.775	0.010	1.236	0.013
114	1:4:51.60	2:10:23.5	17.691	0.012	1.319	0.019
116	1:4:52.00	2:4:19.5	17.312	0.019	1.569	0.027
117	1:4:52.30	2:4:13.4	15.799	0.009	1.488	0.014
118	1:4:52.50	2:4:24.9	16.445	0.013	1.684	0.019
122	1:4:54.20	2:3:44.9	17.100	0.019	1.144	0.023
123	1:4:54.30	2:4:20.6	17.043	0.017	1.460	0.023
125	1:4:56.10	2:7:45.0	16.845	0.009	1.587	0.014
126	1:4:56.20	2:8:2.9	16.559	0.008	1.684	0.014
128	1:4:57.90	2:10:44.4	17.227	0.013	1.251	0.020
129	1:4:58.10	2:2:57.7	16.690	0.015	1.413	0.019
131	1:4:58.60	2:4:26.5	16.396	0.013	1.272	0.017
134	1:4:59.30	2:6:58.7	17.559	0.012	1.083	0.017
135	1:4:59.60	2:9:58.2	16.862	0.010	1.371	0.015
139	1:5:0.70	2:7:10.1	17.282	0.011	2.423	0.027
142	1:5:2.60	2:7:17.8	16.998	0.011	1.384	0.015

Table 3. NIR magnitudes and colours of C stars in NGC 3109.

id	RA	Dec	K_s	σ_K	$J-K_s$	σ_{J-K}
106	10:2:53.17	−26:9:8.2	18.023	0.031	1.255	0.048
108	10:2:53.92	−26:10:20.1	17.550	0.037	1.531	0.056
109	10:2:54.11	−26:10:33.2	17.514	0.043	1.532	0.056
111	10:2:54.29	−26:9:57.8	18.843	0.040	1.163	0.047
112	10:2:54.59	−26:10:2.5	18.081	0.025	1.513	0.029
113	10:2:54.74	−26:8:52.1	18.477	0.035	1.260	0.043
116	10:2:54.90	−26:10:34.8	18.586	0.038	1.278	0.048
117	10:2:55.24	−26:9:13.0	18.302	0.023	1.154	0.026
118	10:2:55.40	−26:9:19.2	18.868	0.033	1.153	0.038
119	10:2:55.42	−26:10:59.8	17.997	0.038	1.382	0.054
122	10:2:55.95	−26:8:37.6	18.403	0.045	1.108	0.060
123	10:2:56.59	−26:8:54.7	17.477	0.021	1.797	0.028
124	10:2:56.73	−26:9:13.3	17.747	0.020	1.501	0.033
126	10:2:56.94	−26:9:7.5	17.497	0.025	2.814	0.033
127	10:2:57.09	−26:9:39.0	17.659	0.018	1.869	0.024
128	10:2:57.12	−26:9:22.0	18.738	0.033	2.168	0.048
130	10:2:57.24	−26:9:46.2	18.353	0.022	1.428	0.032
132	10:2:57.79	−26:8:38.2	17.535	0.032	1.990	0.043
134	10:2:58.09	−26:9:18.9	17.016	0.020	1.715	0.033
135	10:2:58.38	−26:8:56.9	17.318	0.016	1.809	0.023
136	10:2:58.42	−26:10:46.8	18.347	0.029	1.297	0.034
137	10:2:58.92	−26:9:49.6	18.002	0.024	1.446	0.036
138	10:2:58.95	−26:9:7.5	19.133	0.038	1.033	0.045
139	10:2:58.99	−26:9:17.7	18.673	0.018	1.148	0.023
142	10:2:59.39	−26:10:46.5	17.744	0.029	1.712	0.036
143	10:2:59.46	−26:8:39.3	17.321	0.022	1.412	0.030
145	10:2:59.49	−26:9:18.8	17.315	0.018	1.805	0.027
146	10:3:0.01	−26:8:54.1	18.124	0.027	1.280	0.034
147	10:3:0.02	−26:8:44.3	16.686	0.022	1.858	0.030
148	10:3:0.07	−26:10:12.2	18.603	0.031	1.239	0.036
150	10:3:0.47	−26:8:37.2	17.478	0.037	1.629	0.062
151	10:3:0.70	−26:10:12.7	17.126	0.019	1.668	0.030
152	10:3:0.77	−26:8:56.0	17.136	0.018	1.208	0.028
154	10:3:0.89	−26:8:47.6	17.266	0.019	1.440	0.026
156	10:3:1.01	−26:8:43.2	18.571	0.027	1.287	0.038
157	10:3:1.11	−26:9:19.2	18.216	0.025	1.625	0.035
158	10:3:1.13	−26:8:47.3	17.847	0.018	1.415	0.031
159	10:3:1.43	−26:8:51.7	17.525	0.018	1.281	0.024
160	10:3:1.49	−26:10:23.4	18.543	0.032	1.233	0.041
161	10:3:1.52	−26:9:1.2	17.101	0.023	1.640	0.029
163	10:3:1.80	−26:9:32.5	18.282	0.031	1.212	0.038
164	10:3:1.86	−26:8:51.0	17.830	0.031	1.973	0.049
165	10:3:1.98	−26:10:32.7	18.330	0.041	1.538	0.049
166	10:3:2.01	−26:9:10.6	17.798	0.021	1.814	0.029
168	10:3:2.46	−26:9:33.4	17.928	0.019	1.519	0.027
169	10:3:2.59	−26:8:41.9	17.907	0.040	1.604	0.051
170	10:3:2.65	−26:9:22.3	17.289	0.020	1.590	0.027
170	10:3:2.65	−26:9:22.3	17.516	0.033	1.454	0.045
171	10:3:2.69	−26:8:45.8	18.745	0.046	1.152	0.059
172	10:3:2.74	−26:9:11.4	17.379	0.032	1.413	0.044
176	10:3:3.14	−26:8:55.4	18.135	0.037	1.259	0.050
177	10:3:3.19	−26:10:18.6	19.067	0.032	1.256	0.045
177	10:3:3.19	−26:10:18.6	19.170	0.054	1.234	0.061
178	10:3:3.21	−26:9:43.4	18.826	0.030	1.277	0.037
179	10:3:3.28	−26:9:34.1	18.826	0.046	1.276	0.057
180	10:3:3.31	−26:9:1.8	17.747	0.033	1.576	0.043
180	10:3:3.31	−26:9:1.8	17.809	0.045	1.591	0.063
181	10:3:3.38	−26:9:43.5	18.048	0.021	1.275	0.026
181	10:3:3.38	−26:9:43.5	18.133	0.036	1.212	0.045
182	10:3:3.53	−26:9:58.6	16.647	0.022	1.599	0.033
182	10:3:3.53	−26:9:58.6	16.770	0.039	1.448	0.047
183	10:3:3.53	−26:10:12.3	17.690	0.026	1.671	0.033
183	10:3:3.53	−26:10:12.3	17.795	0.025	1.672	0.033
184	10:3:3.66	−26:9:15.7	17.871	0.036	1.366	0.041
185	10:3:3.95	−26:8:58.2	17.390	0.052	1.603	0.066

Table 3. continued.

id	RA	Dec	K_s	σ_K	$J-K_s$	σ_{J-K}
185	10:3:3.95	−26:8:58.2	17.473	0.065	1.545	0.076
187	10:3:4.14	−26:8:34.8	18.120	0.059	1.231	0.090
188	10:3:4.27	−26:8:56.6	18.417	0.032	1.207	0.051
191	10:3:4.59	−26:9:38.3	17.859	0.035	1.216	0.044
192	10:3:5.01	−26:9:0.0	17.460	0.047	1.752	0.055
196	10:3:5.74	−26:11:24.9	17.325	0.035	1.247	0.046
197	10:3:6.19	−26:8:57.4	17.501	0.050	1.771	0.059
199	10:3:6.42	−26:9:0.3	17.362	0.043	1.933	0.049
203	10:3:8.07	−26:9:4.8	17.410	0.034	1.975	0.037
204	10:3:8.13	−26:10:40.7	18.088	0.038	1.912	0.046
205	10:3:8.28	−26:9:18.6	17.402	0.027	1.206	0.032
208	10:3:8.42	−26:9:6.1	17.368	0.035	1.829	0.043
209	10:3:8.98	−26:10:24.2	17.863	0.029	1.427	0.033
211	10:3:8.99	−26:10:2.3	17.826	0.039	2.425	0.043
213	10:3:9.10	−26:8:59.9	17.784	0.039	1.603	0.047
216	10:3:9.41	−26:9:8.5	17.756	0.030	1.458	0.038
217	10:3:9.51	−26:10:26.6	17.429	0.026	1.760	0.030
218	10:3:9.53	−26:10:33.3	17.463	0.029	1.587	0.032
219	10:3:9.56	−26:9:1.2	18.109	0.032	1.418	0.037
222	10:3:9.70	−26:9:13.1	16.850	0.029	1.331	0.034
223	10:3:9.88	−26:9:16.6	18.250	0.024	1.213	0.033
224	10:3:9.91	−26:10:17.5	18.015	0.039	1.274	0.047
225	10:3:10.11	−26:9:22.8	16.875	0.024	1.637	0.030
226	10:3:10.15	−26:9:31.1	18.577	0.027	1.121	0.035
228	10:3:10.44	−26:10:31.8	17.552	0.034	1.500	0.038
229	10:3:10.68	−26:10:17.1	17.736	0.022	1.698	0.029
230	10:3:10.75	−26:9:31.2	18.244	0.025	1.469	0.033
232	10:3:10.96	−26:9:17.0	17.950	0.034	1.207	0.040
233	10:3:11.07	−26:9:16.1	17.813	0.030	1.724	0.035
236	10:3:11.40	−26:9:11.8	17.273	0.047	1.489	0.051
237	10:3:11.41	−26:9:25.6	18.158	0.048	1.691	0.053
239	10:3:11.49	−26:9:23.8	17.840	0.031	1.713	0.037
240	10:3:11.78	−26:10:39.7	17.943	0.038	2.019	0.048
241	10:3:11.86	−26:8:57.8	17.614	0.077	1.629	0.087
242	10:3:11.87	−26:10:14.8	17.240	0.026	1.646	0.032
243	10:3:11.97	−26:9:38.3	17.221	0.026	1.357	0.032
244	10:3:11.98	−26:9:18.4	17.565	0.037	1.950	0.043
245	10:3:11.99	−26:9:50.3	17.656	0.032	1.621	0.040
247	10:3:12.39	−26:9:35.7	16.910	0.030	1.811	0.036
249	10:3:12.67	−26:9:45.6	18.671	0.041	1.206	0.049
251	10:3:12.82	−26:9:31.2	17.028	0.046	1.642	0.053
252	10:3:12.84	−26:9:33.8	17.961	0.054	1.515	0.060
253	10:3:12.84	−26:9:49.3	17.772	0.043	1.529	0.048
254	10:3:12.90	−26:9:1.5	17.400	0.089	2.031	0.107
256	10:3:12.97	−26:9:15.6	17.268	0.069	1.781	0.077
257	10:3:13.10	−26:10:48.4	17.965	0.046	2.719	0.058
258	10:3:13.12	−26:9:28.0	16.384	0.069	1.893	0.078
259	10:3:13.18	−26:9:26.7	17.382	0.049	1.740	0.061
260	10:3:13.35	−26:9:52.6	17.344	0.022	1.640	0.039
261	10:3:13.36	−26:10:30.6	17.483	0.039	1.914	0.048
261	10:3:13.36	−26:10:30.6	17.495	0.036	1.903	0.050
262	10:3:13.43	−26:9:14.0	18.121	0.084	1.698	0.099
265	10:3:13.84	−26:10:12.7	16.742	0.029	1.767	0.040
268	10:3:14.10	−26:10:38.8	17.783	0.045	1.776	0.056
269	10:3:14.12	−26:10:15.4	17.044	0.029	1.845	0.040
273	10:3:14.92	−26:10:20.6	17.183	0.020	1.489	0.031
274	10:3:14.95	−26:9:46.6	18.113	0.080	1.393	0.103
275	10:3:15.10	−26:10:4.7	18.074	0.026	1.343	0.044
276	10:3:15.35	−26:10:39.9	18.368	0.027	1.788	0.040
281	10:3:15.72	−26:10:38.4	17.781	0.048	1.562	0.062
283	10:3:15.89	−26:10:3.9	17.156	0.026	1.836	0.037

Table 3. continued.

id	RA	Dec	K_s	σ_K	$J-K_s$	σ_{J-K}
285	10:3:15.98	−26:9:21.6	17.394	0.017	1.770	0.085
287	10:3:16.08	−26:10:24.7	17.325	0.029	2.110	0.037
288	10:3:16.12	−26:10:49.3	17.695	0.026	1.829	0.039
291	10:3:16.48	−26:9:35.3	18.807	0.072	0.933	0.090
295	10:3:17.06	−26:9:44.2	17.903	0.024	1.234	0.036
297	10:3:17.28	−26:10:27.4	18.153	0.025	1.597	0.040
304	10:3:18.07	−26:10:8.1	17.637	0.026	2.208	0.049
308	10:3:18.43	−26:11:1.8	17.233	0.023	1.821	0.031
311	10:3:18.61	−26:10:27.1	17.726	0.020	2.135	0.035
316	10:3:19.05	−26:9:23.1	17.057	0.020	2.195	0.060
324	10:3:19.95	−26:8:58.4	17.394	0.018	2.167	0.028
325	10:3:20.03	−26:10:9.0	17.120	0.019	1.848	0.039
327	10:3:20.07	−26:10:10.1	17.001	0.016	1.529	0.032
328	10:3:20.12	−26:10:11.1	18.478	0.023	1.553	0.056
329	10:3:20.16	−26:10:31.1	17.389	0.023	2.146	0.049
331	10:3:20.66	−26:10:2.7	17.446	0.018	1.819	0.027
340	10:3:21.76	−26:10:2.7	17.602	0.024	1.586	0.039
341	10:3:21.86	−26:10:41.9	17.931	0.025	2.075	0.037
342	10:3:21.89	−26:11:4.9	17.253	0.048	2.093	0.057
343	10:3:22.05	−26:9:33.5	18.431	0.033	1.276	0.042
344	10:3:22.18	−26:10:17.0	17.825	0.019	1.701	0.030
345	10:3:22.23	−26:9:11.9	17.067	0.026	2.059	0.036
348	10:3:22.40	−26:10:4.0	17.845	0.025	1.626	0.033
354	10:3:22.91	−26:10:10.7	18.130	0.016	1.753	0.032
357	10:3:23.37	−26:10:2.8	18.453	0.027	1.233	0.041
358	10:3:23.74	−26:11:9.0	18.421	0.062	1.633	0.100
360	10:3:23.85	−26:10:17.7	18.657	0.026	1.472	0.043
361	10:3:23.95	−26:10:34.1	18.107	0.042	1.781	0.058
364	10:3:24.08	−26:10:40.2	17.842	0.036	1.610	0.048
366	10:3:24.37	−26:8:54.1	18.712	0.070	1.179	0.083
367	10:3:24.49	−26:10:52.1	18.145	0.049	1.658	0.085